Design and Synthesis of Peptidomimetic Factor VIIa Inhibitors

Takuya Shiraishi,* Shojiro Kadono, Masayuki Haramura, Hirofumi Kodama, Yoshiyuki Ono, Hitoshi Iikura, Tohru Esaki, Takaki Koga, Kunihiro Hattori, Yoshiaki Watanabe, Akihisa Sakamoto, Kazutaka Yoshihashi, Takehisa Kitazawa, Keiko Esaki, Masateru Ohta, Haruhiko Sato, and Toshiro Kozono

Fuji Gotemba Research Laboratories, Chugai Pharmaceutical Co., Ltd.; 1–135 Komakado, Gotemba, Shizuoka 412–8513, Japan. Received July 25, 2009; accepted October 10, 2009; published online October 15, 2009

Selective factor VIIa-tissue factor complex (FVIIa/TF) inhibition is regarded as a promising target for developing new anticoagulant drugs. In previous reports, we described a S3 subsite found in the X-ray crystal structure of compound 2 that bound to FVIIa/soluble tissue factor (sTF). Based on the X-ray crystal structure information and with the aim of improving the inhibition activity for FVIIa/TF and selectivity against other serine proteases, we synthesized derivatives by introducing substituents at position 5 of the indole ring of compound 2. Among them, compound 16 showed high selectivity against other serine proteases. Contrary to our expectations, compound 16 did not occupy the S3-subsite; X-ray structure analysis revealed that compound 16 improved selectivity by forming hydrogen bonds with Gln217, Thr99 and Asn100.

Key words factor VIIa; X-ray; 2×activated partial thromboplastin time/2×prothrombin time; thromboembolic disorder; peptidomimetic inhibitor

Coagulation factor VIIa (FVIIa; EC 3.4.21.21) is a serine protease enzyme which plays an important role in the blood coagulation cascade comprising extrinsic and intrinsic coagulation pathways. FVIIa in complex with tissue factor (TF) (FVIIa/TF) initiates the extrinsic coagulation pathway. The extrinsic pathway is triggered by formation of the complex, which subsequently activates factor IX to IXa and factor X to Xa, which in turn activates factor X to Xa and prothrombin to thrombin, respectively.[1] Thrombin cleaves fibrinogen to fibrin, which forms blood clots with activated platelets. Inappropriate thrombus formation in blood vessels causes cardiovascular diseases (myocardial infarction, stroke, pulmonary embolism, *etc.*), which are the most common causes of mortality in industrialized countries.[2] Recent studies on blood coagulation have suggested that selective inhibition of extrinsic coagulation provides effective anticoagulation and low risk of bleeding compared with other antithrombotic mechanisms.[3—8] Therefore, specific inhibition of FVIIa/TF and thus extrinsic coagulation is expected to be a promising target in the development of new anticoagulant drugs.[9—17]

Recently, we reported a peptidomimetic FVIIa inhibitor (**2**) with a Gln moiety as the P2 from optimization of thrombin inhibitor **1** at the substituents to the S2 and S3 pocket (Fig. 1).[18—25] The X-ray structure of **2** suggested that the glutamine side chain forms potent hydrogen bonds with Asp60, Tyr94, and Thr98 in the hydrophilic pocket of the S2 site of FVIIa/sTF.[18—24] Surprisingly, in the case of compound **2**, there appears to be a hole extendable to the space near the S3 site (Fig. 2) not observed upon binding to D-Phe-Phe-Arg-chloromethyl-ketone.[19,21,26]

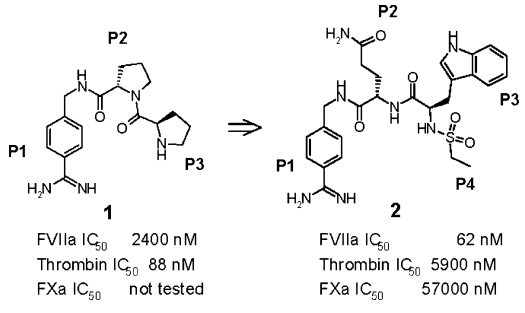

Fig. 1. Structure of Compounds **1** and **2**

This condition is caused by the change in the Gln217 side chain when the indole ring of compound **2** binds to a specific position in the S3 site. A channel was found near position 5 of the indole ring in P3 and, through this channel, it might be possible to access the large cavity consisting of Cys168, Ile176, Cys182, His224, Phe225, Gly226, and Val227 (the S3 subsite). This large cavity exists only in FVIIa/TF because, among the coagulation serine proteases, only FVIIa has a large 170-loop. Therefore, the introduction of the appropriate substituent at position 5 of the indole ring of compound **2** was expected to lead to new interactions with the S3 subsite through this channel and to improve the binding affinity and selectivity for FVIIa/TF.

Chemistry The typical synthetic route for our compounds is shown in Chart 1. Intermediate **9** was prepared by starting with condensation of 4-cyanobenzylamine (**3**) and

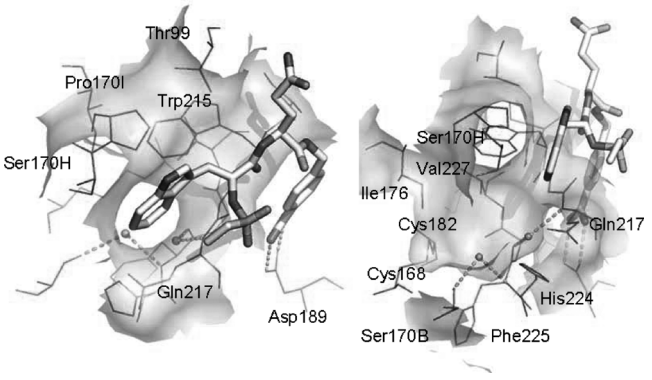

Fig. 2. Crystal Structure of Compound **2** Bound to FVIIa/sTF (PDB 1WUN)

The figure on the left shows the molecular surface around the S4 site. Near position 5 of the indole moiety at P3 of compound **2**, a tunnel through which it is possible to connect an internal large cavity form S4 site was found. The figure on the right shows the internal cavity in which two fixed water molecules were found.

* To whom correspondence should be addressed. e-mail: shiraishitky@chugai-pharm.co.jp

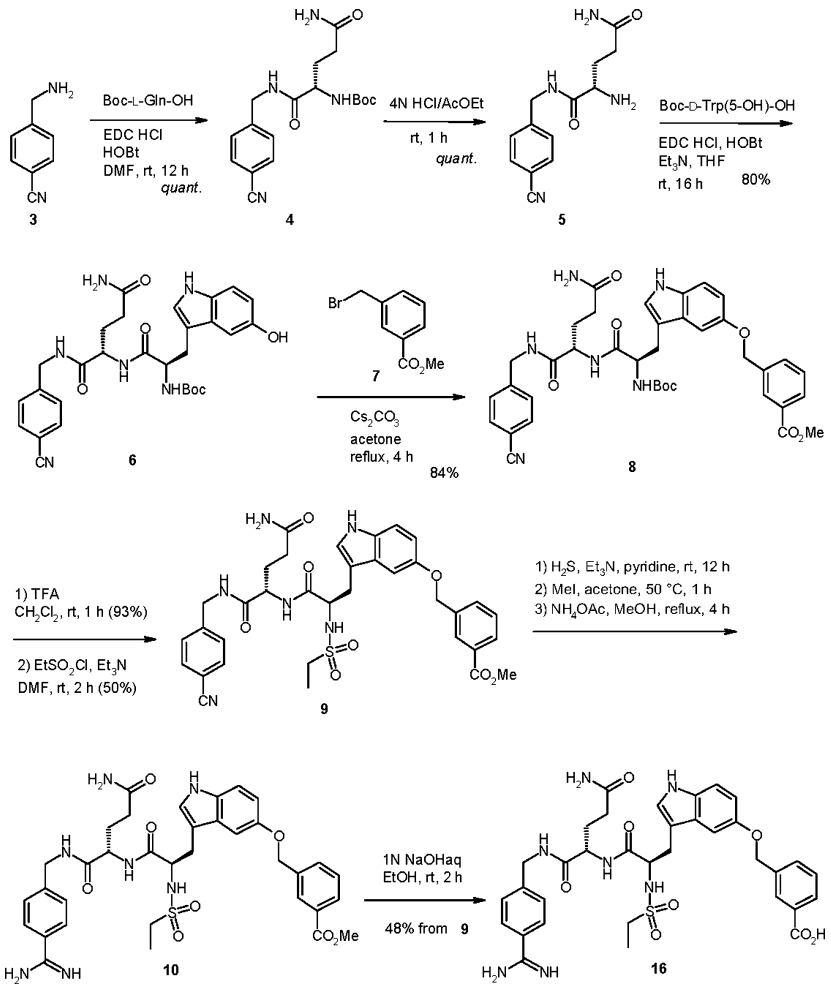

Chart 1. Synthesis of Compound **16**

Boc-L-Gln under 1-ethyl-3-(3-dimethylaminopropyl) carbodiimide (EDC)/1-hydroxybenzotriazole (HOBt) conditions. After cleavage of the Boc-protecting group and the condensation amine (**5**) with Boc-D-Trp(5-OH) under EDC/HOBt conditions, compound **6** was reacted with 3-substituted benzyl bromide (**7**). After cleavage of the Boc-protecting group, the reaction of the amine with ethanesulfonyl chloride led to intermediate **9**. The nitrile was converted to the amidine and hydrolysis of the ester led to the desired product **16**. The other compounds were prepared following the same procedure.

Results and Discussion

Based on the crystal structure, the NH at position 1 of the indole ring of D-tryptophan is exposed to the solvent and does not appear to contribute to the binding of FVIIa/TF. This is supported by the fact that the introduction of a Me group to the nitrogen of the indole ring of compound **2** results in conservation of the affinity for FVIIa/TF, as shown in Table 1. However, thrombin and FXa have hydrophobic S3 pockets so the increased hydrophobicity of the indole ring by the introduction of a Me group at position 1 of the indole ring of compound **2** reduced selectivities against thrombin and factor Xa.

In the crystal structure of FVIIa/soluble tissue factor (sTF) bound to compound **2**, the channel observed near position 5 of the indole ring has hydrophobic residues near the gate. This is supported by the fact that the introduction of an OH moiety to position 5 of the indole ring of compound **2** resulted in a decrease in the FVIIa/TF binding affinity; however, the introduction of an OMe moiety to the same position resulted in regaining the FVIIa/TF binding affinity to the same level exhibited by compound **2**.

Based on the crystal structure of FVIIa/sTF bound to compound **2**, which has the propoxy group at position 5 of the indole ring in P3, we synthesized compound **14**. Compound **14** showed improved coagulation over other serine proteases. We tested compound **14** using standard clotting assays including a prothrombin time (PT) assay and an activated partial thromboplastin time (APTT) assay to confirm the improved specificity for FVIIa/TF inhibition. Theoretically, specific inhibition of FVIIa/TF, which blocks only extrinsic coagulation, should result in prolongation of only PT without affecting APTT, thus making the concentration ratio for twofold prolongations of APTT and PT (2×APTT/2×PT) infinitely large. The measured 2×APTT/2×PT ratio of compound **14** was 15.9, higher than that of compound **2** (6.1). To confirm the binding mode of compound **14** to FVIIa/TF, the crystal structure bound to FVIIa/sTF was solved by X-ray crystallography (Fig. 3). Unfortunately, the expected binding with the S3 subsite was not found.

The binding mode of compound **14** is basically the same

Table 1. Inhibition of FVIIa/TF and Related Serine Proteases from Compounds **2**, **11**—**16**

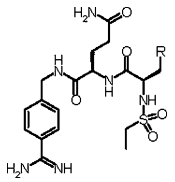

Compound	R	IC_{50} (nM)							2×APTT/ 2×PT
		FVIIa	Thrombin	FXa	FIXa	FXIa	FXIIa	aPC	
2		62	5900	57000	>100000	270	79000	2900	6.1
11		69	1400	3700	>100000	210	38000	2100	2.0
12	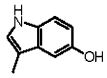	140	13000	>100000	NT[a)]	1600	NT[a)]	3600	8.6
13	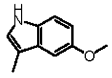	65	8300	>100000	NT[a)]	2600	NT[a)]	3500	14.0
14	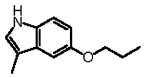	56	14000	>100000	>100000	3100	>100000	4000	15.9
15	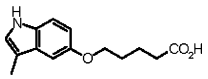	204	19000	>100000	NT[a)]	NT[a)]	NT[a)]	7400	NT[a)]
16	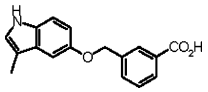	39	18000	>100000	NT[a)]	4700	NT[a)]	4800	28.1

a) Not tested.

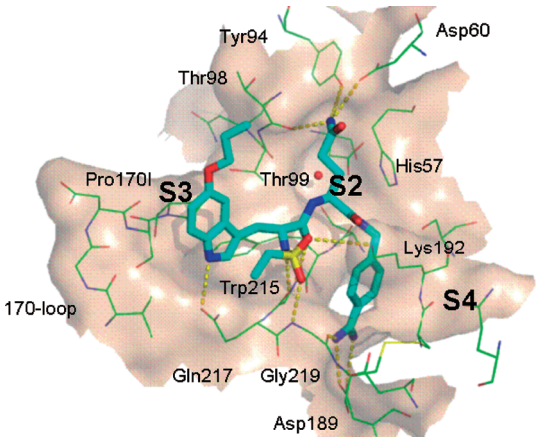

Fig. 3. Crystal Structure of Compound **14** Bound to FVIIa/sTF (PDB 1WV7)

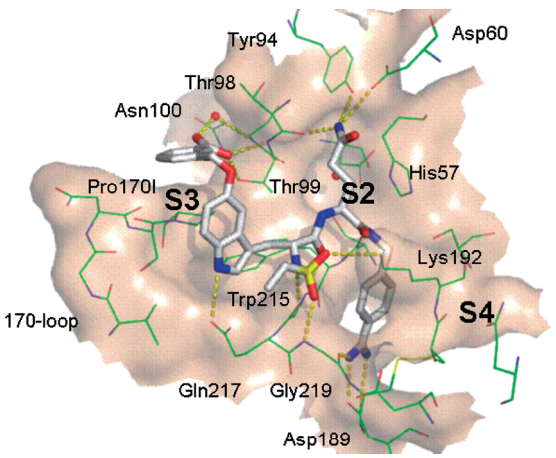

Fig. 4. Crystal Structure of Compound **16** Bound to FVIIa/sTF (PDB 2ZZU)

as that of compound **2**. However, the 5-propoxy-indole moiety in P3 of compound **14** is accommodated in the S3 site in a far different binding mode than for the non-substituted indole moiety in P3 of compound **2**. Surprisingly, the 5-propoxy-indole moiety flips and the propoxy moiety extends to the solvent region. As a result of this conformation, the hydrophobic interactions with Gln217 and 170-loop are lost. However, a new hydrogen bond between the NH of the indole ring and Gln217 was observed. Among coagulation serine proteases, only Gln217 of FVIIa has a uniquely bent conformation, which makes possible a hydrogen bond with the NH of the indole.

The abovementioned occupation of the S3 subsite by simple hydrophobic substituents was not successful. In another

approach to the forming of new interactions with the S3 subsite, we focused on water molecules. In the crystal structures of FVIIa/sTF bound to our compounds, two highly conserved water molecules were observed in the S3 subsite. One formed hydrogen bonds with Ser170B and Phe225, and the other formed hydrogen bonds with Gln217 and Phe225. Compounds **15** and **16** were designed by replacing these water molecules.

As shown in Table 1, compound **15** showed less activity than compound **2**. However, compound **16** showed improved activity over compound **2** with a slight amelioration of selectivities against other serine proteases and an improved 2×APTT/2×PT ratio (28.1) compared with compound **2**. We concluded that compound **16** achieves higher selectivity for extrinsic coagulation inhibition.

To confirm the binding mode of compound **16** to FVIIa/TF, the crystal structure bound to FVIIa/sTF was solved by X-ray crystallography (Fig. 4). In this structure, the expected binding with the S3 subsite was not observed. The binding of compound **16** to FVIIa/sTF was almost the same as that of compound **14**. The NH of the indole in the P3 moiety formed a hydrogen bond with Gln217. Additionally, the benzyl carboxylate moiety stacks on Pro170I. The carboxylate formed hydrogen bonds with the Thr99 side chain OH and the main chain NH atoms. And this carboxylate formed a hydrogen bond with the Asn100 main chain NH atom through a water molecule. Of the other coagulation serine proteases, Thr99 is not conserved and FVIIa and aPC have Thr in this sequence position. However, the main chain conformation near this residue was completely different between FVIIa and aPC. Only FVIIa can form these hydrogen bonds with the carboxylate of the ligand. Hence, these interactions contribute to the improvement of selectivity to FVIIa.

Conclusion

We have designed and synthesized peptidomimetic FVIIa inhibitors based on the X-ray crystallographic structure of compound **2**. Among these compounds, compound **16** showed the highest selectivity and a high 2×APTT/2×PT ratio (28.1). X-Ray structure analysis revealed that compound **16** exhibited improved selectivity by forming unexpected hydrogen bonds with Gln217, Thr99 and Asn100. This structural information will be of benefit to the development of FVIIa-specific inhibitors.

Experimental

Chemistry In general, reagents and solvents were used as purchased without further purification. Column chromatography was carried out on Merck silica gel 60 (230—400 mesh) if not otherwise specified. ^{1}H-NMR spectra were recorded on JEOL EX-270, JEOL ECP-400 or a Mercury 300 MHz instrument in $CDCl_3$, DMSO-d_6 or CD_3OD solutions. Low resolution mass spectra were determined on an LC/photodiode array (PDA)/MS (HP 1100/TSP UV 6000/LCQ Classic, LCMS) system using Cadenza CD-C18 column (3.0 mm i.d.×20 mm) at 35 °C. The accurate mass of the target compound was measured using an Agilent 1100 series (Agilent Technologies, Inc. Santa Clara, CA, U.S.A.) and QSTAR XL system (Applied Biosystems/MDS Analytical Technologies, Toronto, Canada) in the electrospray ionization (ESI) positive ion mode. The sample solution was separated using an Inertsil octadecyl silica (ODS)-3.3 μm column (4.0 mm i.d.×33 mm; GL Science) at 30 °C.

[(*S*)-3-Carbamoyl-1-(4-cyano-benzylcarbamoyl)-propyl]-carbamic Acid *tert*-Butyl Ester (4) To a solution of 4-aminomethyl-benzonitrile (1.6 g, 12.2 mmol) in *N*,*N*-dimethylformamide (DMF) (20 ml), *tert*-butoxycarbonyl-L-glutamine (2.0 g, 8.1 mmol), 1-hydroxybenzotriazole (HOBt) (1.4 g, 8.9 mmol) and 1-ethyl-3-(3-dimethylaminopropyl)carbodiimide hydrochloride (EDC HCl) (1.7 g, 8.9 mmol) were added and stirred at room temperature under a nitrogen stream. After 12 h, water was added to the reaction mixture, which was then extracted with ethyl acetate. The ethyl acetate layer was washed sequentially with 10% aqueous citric acid, saturated aqueous sodium bicarbonate and saturated brine, and then dried over anhydrous magnesium sulfate. The magnesium sulfate was filtered off and the filtrate was concentrated under reduced pressure to give **4** (2.9 g, quant.) as a colorless solid. ^{1}H-NMR (400 MHz, CD_3OD) δ: 1.45 (9H, s), 1.83—2.10 (2H, m), 2.31 (2H, d, J=7.6 Hz), 4.06 (1H, dd, J=4.9, 8.8 Hz), 4.46 (2H, dd, J=15.6, 20.0 Hz), 7.47 (2H, d, J=8.3 Hz), 7.67 (2H, d, J=8.3 Hz); ESI+ 383 $[M+Na]^+$.

(*S*)-2-Amino-pentanedioic Acid 5-Amide 1-(4-Cyano-benzylamide) (5) To **4** (2.9 g, 8.1 mmol), a solution of 4 N hydrogen chloride/ethyl acetate (20 ml) was added and stirred at room temperature under a nitrogen stream. After 1 h, the solvent was distilled off under reduced pressure and the residue was applied to column chromatography (Fuji Silysia NH-DM-1020; mobile phase: dichloromethane : methanol=1 : 1) to give **5** (2.1 g, quant.) as a colorless solid. ^{1}H-NMR (400 MHz, CD_3OD) δ: 1.78—2.03 (2H, m), 2.29 (2H, t, J=7.8 Hz), 3.38 (1H, dd, J=5.9, 7.8 Hz), 4.47 (2H, s), 7.48 (2H, d, J=8.3 Hz), 7.69 (2H, d, J=8.3 Hz); ESI− 259 (M^+-1).

[(*R*)-1-[(*S*)-3-Carbamoyl-1-(4-cyano-benzylcarbamoyl)-propylcarbamoyl]-2-(5-hydroxy-1*H*-indol-3-yl)-ethyl]-carbamic Acid *tert*-Butyl Ester (6) To a stirred suspension of **5** (510 mg, 1.96 mmol) and *tert*-butoxycarbonyl-D-(5-hydroxy)tryptophan (624 mg, 1.96 mmol) in THF (50 ml) was added HOBt (345 mg, 2.55 mmol), EDC HCl (488 mg, 2.55 mmol) and triethylamine (480 mg, 4.71 mmol) and stirred at room temperature under a nitrogen stream. After 15 h, water was added to the reaction mixture, which was then extracted with ethyl acetate. The ethyl acetate layer was washed sequentially with saturated aqueous ammonium chloride, saturated aqueous sodium bicarbonate and saturated brine, and then dried over sodium sulfate. The sodium sulfate was filtered off and the filtrate was concentrated under reduced pressure. The residue was applied to flash column chromatography (Merck silica gel 60; mobile phase: dichloromethane : methanol=10 : 0 to 9 : 1) to give **6** (882 mg, 80%). ^{1}H-NMR (300 MHz, DMSO-d_6) δ: 1.25 (9H, s), 1.60—2.03 (4H, m), 2.70—3.02 (2H, m), 4.08—4.45 (4H, m), 6.58 (1H, dd, J=1.8, 8.3 Hz), 6.74 (1H, br s), 6.88 (1H, d, J=5.3 Hz), 6.98 (1H, d, J=5.9 Hz), 7.06 (1H, d, J=1.8 Hz), 7.10 (1H, d, J=8.3 Hz), 7.42 (2H, d, J=7.3 Hz), 7.76 (2H, d, J=7.3 Hz); ESI+ 563 (M^++1).

3-(3-{(*R*)-2-*tert*-Butoxycarbonylamino-2-[(*S*)-3-carbamoyl-1-(4-cyano-benzylcarbamoyl)-propylcarbamoyl]-ethyl}-1*H*-indol-5-yloxymethyl)-benzoic Acid Methyl Ester (8) To a solution of **6** (327 mg, 0.58 mmol) in acetone (4 ml), 3-(methoxycarbonyl)benzylbromide (**7**) (267 mg, 1.2 mmol) and cesium carbonate (378 mg, 1.2 mmol) were added and stirred at reflux under a nitrogen stream. After 4 h, the reaction mixture was filtered and the filtrate was concentrated under reduced pressure. The residue was applied to flash column chromatography (Merck silica gel 60; mobile phase: dichloromethane : methanol=10 : 1) to give **8** (347 mg, 84%). ^{1}H-NMR (270 MHz, CD_3OD) δ: 1.28 (9H, s), 1.50—2.05 (4H, m), 3.03—3.19 (2H, m), 3.91 (3H, s), 4.01—4.24 (2H, m), 4.43 (2H, s), 5.19 (2H, s), 6.87 (1H, dd, J=2.2, 8.8 Hz), 7.11 (1H, s), 7.18 (1H, d, J=2.3 Hz), 7.28 (1H, d, J=8.9 Hz), 7.41 (2H, d, J=8.3 Hz), 7.50 (1H, t, J=7.8 Hz), 7.65 (2H, d, J=8.3 Hz), 7.75 (1H, d, J=7.5 Hz), 7.96 (1H, d, J=7.5 Hz), 8.16 (1H, s); ESI+ 711 (M^++1).

3-(3-{(*R*)-2-[(*S*)-3-Carbamoyl-1-(4-cyano-benzylcarbamoyl)-propylcarbamoyl]-2-ethanesulfonylamino-ethyl}-1*H*-indol-5-yloxymethyl)-benzoic Acid Methyl Ester (9) To a solution of **8** (347 mg, 0.5 mmol) in dichloromethane (10 ml), trifluoroacetic acid (10 ml) was added and stirred at room temperature under a nitrogen stream. After 1 h, the solvent was distilled off under reduced pressure. The residue was applied to column chromatography (Fuji Silysia NH-DM-1020; mobile phase: dichloromethane : methanol=1 : 1) to give 3-(3-{(*R*)-2-amino-2-[(*S*)-3-carbamoyl-1-(4-cyano-benzylcarbamoyl)-propylcarbamoyl]-ethyl}-1*H*-indol-5-yloxymethyl)-benzoic acid methyl ester (277 mg, 93%).

To a solution of 3-(3-{(*R*)-2-amino-2-[(*S*)-3-carbamoyl-1-(4-cyano-benzylcarbamoyl)-propylcarbamoyl]-ethyl}-1*H*-indol-5-yloxymethyl)-benzoic acid methyl ester (0.45 mmol) in DMF (10 ml), triethylamine (137 mg, 1.4 mmol) and ethanesulfonyl chloride (174 mg, 1.4 mmol) were added and stirred at room temperature under a nitrogen stream. After 2 h, the solvent was distilled off under reduced pressure and the residue was applied to flash column chromatography (Merck silica gel 60; mobile phase: dichloromethane : methanol=8 : 1) to give **9** (158 mg, 50%). ^{1}H-NMR (270 MHz, CD_3OD) δ: 0.95 (3H, t, J=7.3 Hz), 1.60—2.05 (4H, m), 2.59—2.84 (2H, m), 2.97—3.27 (2H, m), 3.90 (3H, s), 4.09—4.20 (2H, m), 4.40 (2H, d, J=2.5 Hz), 5.18 (2H, s), 6.88 (1H, dd, J=2.3, 8.7 Hz), 7.14 (1H, s), 7.22

(1H, d, J=2.3 Hz), 7.26 (1H, d, J=8.7 Hz), 7.43 (2H, d, J=8.7 Hz), 7.48 (1H, t, J=7.9 Hz), 7.64 (2H, d, J=8.6 Hz), 7.73 (1H, d, J=8.1 Hz), 7.95 (1H, d, J=7.9 Hz), 8.15 (1H, s); ESI+ 703 (M^++1).

3-(3-{(*R*)-2-[(*S*)-1-(4-Carbamimidoyl-benzylcarbamoyl)-3-carbamoyl-propylcarbamoyl]-2-ethanesulfonylamino-ethyl}-1*H*-indol-5-yloxymethyl)-benzoic Acid Methyl Ester (10) A solution of **9** (158 mg, 0.22 mmol) in pyridine (10 ml) and triethylamine (2 ml) was bubbled with hydrogen sulfide gas. After bubbling for 30 min, the solution was allowed to stand. After 12 h, water/ethyl acetate was added to the reaction mixture and the aqueous layer was adjusted to pH 4 with 2 N aqueous hydrogen chloride, followed by extraction. The organic layer was washed with saturated brine and then dried over anhydrous magnesium sulfate. The magnesium sulfate was filtered off and the filtrate was concentrated under reduced pressure.

The residue was dissolved in acetone (10 ml), to which methyl iodide (312 mg, 2.2 mmol) was then added and stirred at 50 °C under a nitrogen stream. After 1 h, the reaction mixture was concentrated under reduced pressure.

The residue was dissolved again in methanol (10 ml), followed by the addition of ammonium acetate (170 mg, 2.2 mmol) and heating to reflux under a nitrogen stream. After 4 h, the solvent was distilled off under reduced pressure and the residue was applied to column chromatography (Fuji Silysia NH-DM-1020; mobile phase: dichloromethane : methanol=4 : 1, 2 : 1) to give **10** (124 mg, 78%). ^{1}H-NMR (270 MHz, CD_3OD) δ: 0.94 (3H, t, J=7.4 Hz), 1.63—2.06 (4H, m), 2.54—2.79 (2H, m), 2.96—3.27 (2H, m), 3.89 (3H, s), 4.08—4.21 (2H, m), 4.40 (2H, s), 5.18 (2H, s), 6.87 (1H, dd, J=2.5, 8.7 Hz), 7.15 (1H, s), 7.23 (1H, s), 7.25 (1H, d, J=11.7 Hz), 7.40 (2H, d, J=8.4 Hz), 7.48 (1H, t, J=7.7 Hz), 7.68 (2H, d, J=8.4 Hz), 7.72 (1H, d, J=7.7 Hz), 7.94 (1H, d, J=7.7 Hz), 8.14 (1H, s); ESI+ 720 (M^++1).

3-(3-{(*R*)-2-[(*S*)-1-(4-Carbamimidoyl-benzylcarbamoyl)-3-carbamoyl-propylcarbamoyl]-2-ethanesulfonylamino-ethyl}-1*H*-indol-5-yloxymethyl)-benzoic Acid Trifluoroacetate (16) To a solution of **10** (124 mg, 0.17 mmol) in ethanol (3 ml), 1 N aqueous sodium hydroxide (3 ml) was added and stirred at room temperature. After 2 h, the reaction mixture was adjusted to pH 6 with 1 N aqueous hydrogen chloride and then concentrated under reduced pressure. The residue was applied to preparative HPLC (YMC-pack ODS: gradient of 95% A/B to 25% A/B over 10 min, A=0.1% trifluoroacetic acid (TFA)-H_2O, B=0.1% TFA-CH_3CN) to give **16** (85 mg, 61%). ^{1}H-NMR (270 MHz, CD_3OD) δ: 0.97 (3H, t, J=7.3 Hz), 1.59—2.06 (4H, m), 2.60—2.86 (2H, m), 2.98—3.28 (2H, m), 4.09—4.20 (2H, m), 4.35—4.54 (2H, m), 5.19 (2H, s), 6.89 (1H, dd, J=2.3, 8.7 Hz), 7.15 (1H, s), 7.23 (1H, d, J=2.3 Hz), 7.27 (1H, d, J=8.9 Hz), 7.50 (3H, d, J=8.4 Hz), 7.73 (3H, d, J=8.4 Hz), 7.97 (1H, d, J=7.9 Hz), 8.16 (1H, s); HR-MS (ESI+) Calcd for $C_{34}H_{40}N_7O_8S$: 706.2653 (M^++1). Found: 706.2664.

Nitrile intermediates were prepared using the same methods described above for the synthesis of **9**.

(*S*)-2-[(*R*)-2-Ethanesulfonylamino-3-(1-methyl-1*H*-indol-3-yl)-propionylamino]-pentanedioic Acid 5-Amide 1-(4-Carbamimidoyl-benzylamide) (11) (*S*)-2-[(*R*)-2-Ethanesulfonylamino-3-(1-methyl-1*H*-indol-3-yl)-propionylamino]-pentanedioic acid 5-amide 1-(4-cyano-benzylamide) (77 mg, 0.14 mmol) was dissolved in saturated hydrogen chloride-ethanol solution (10 ml) and allowed to stand at room temperature for 23 h. After the solvent was removed under reduced pressure, the residue was dissolved in ethanol (2 ml) and further dissolved in ammonium acetate (190 mg, 2.4 mmol) and saturated ammonia-ethanol solution (1 ml), followed by heating at reflux. After 2 h, the solvent was distilled off under reduced pressure and the residue was applied to column chromatography (Fuji Silysia NH-DM-1020; mobile phase: dichloromethane : methanol=3 : 1, 1 : 1) to give **11** (23 mg, 29%). ^{1}H-NMR (270 MHz, CD_3OD) δ: 1.00 (3H, t, J=7.4 Hz), 1.42—2.03 (4H, m), 2.61—2.92 (2H, m), 2.98—3.28 (2H, m), 3.74 (3H, s), 4.13—4.21 (2H, m), 4.41 (2H, s), 7.05 (1H, d, J=7.9 Hz), 7.08 (1H, s), 7.17 (1H, t, J=8.3 Hz), 7.32 (1H, d, J=7.9 Hz), 7.42 (2H, d, J=8.3 Hz), 7.61 (1H, d, J=7.8 Hz), 7.68 (2H, d, J=8.3 Hz); HR-MS (ESI+) Calcd for $C_{27}H_{36}N_7O_5S$: 570.2493 (M^++1). Found: 570.2513.

(*S*)-2-[(*R*)-2-Ethanesulfonylamino-3-(5-hydroxy-1*H*-indol-3-yl)-propionylamino]-pentanedioic Acid 5-Amide 1-(4-Carbamimidoyl-benzylamide) Trifluoroacetate (12) Compound **12** was synthesized from (*S*)-2-[(*R*)-2-ethanesulfonylamino-3-(5-benzyloxy-1*H*-indol-3-yl)-propionylamino]-pentanedioic acid 5-amide 1-(4-cyano-benzylamide) according the procedure described for **11** (49%, 26 mg). ^{1}H-NMR (270 MHz, CD_3OD) δ: 1.01 (3H, t, J=7.3 Hz), 1.59—2.06 (4H, m), 2.67—2.90 (2H, m), 2.95—3.23 (2H, m), 4.08—4.20 (2H, m), 4.35—4.52 (2H, m), 6.67 (1H, dd, J=2.3, 8.7 Hz), 6.97 (1H, d, J=2.3 Hz), 7.09 (1H, s), 7.17 (1H, t, J=8.7 Hz), 7.49 (2H, d, J=8.4 Hz), 7.72 (2H, d, J=8.4 Hz); HR-MS (ESI+) Calcd for $C_{26}H_{34}N_7O_6S$: 572.2285 (M^++1). Found: 572.2318.

(*S*)-2-[(*R*)-2-Ethanesulfonylamino-3-(5-methoxy-1*H*-indol-3-yl)-propionylamino]-pentanedioic Acid 5-Amide 1-(4-Carbamimidoyl-benzylamide) Trifluoroacetate (13) Compound **13** was synthesized from (*S*)-2-[(*R*)-2-ethanesulfonylamino-3-(5-methoxy-1*H*-indol-3-yl)-propionylamino]-pentanedioic acid 5-amide 1-(4-cyano-benzylamide) according the procedure described for **11** (65%, 68 mg). ^{1}H-NMR (270 MHz, CD_3OD) δ: 1.04 (3H, t, J=7.3 Hz), 1.60—2.08 (4H, m), 2.72—2.92 (2H, m), 3.03—3.31 (2H, m), 3.87 (3H, s), 4.12—4.22 (2H, m), 4.38—4.55 (2H, m), 6.80 (1H, dd, J=2.4, 8.8 Hz), 7.13 (1H, d, J=2.4 Hz), 7.17 (1H, s), 7.26 (1H, d, J=8.9 Hz), 7.53 (2H, d, J=8.6 Hz), 7.76 (2H, d, J=8.6 Hz); HR-MS (ESI+) Calcd for $C_{27}H_{36}N_7O_6S$: 586.2442 (M^++1). Found: 586.2419.

(*S*)-2-[(*R*)-2-Ethanesulfonylamino-3-(5-propoxy-1*H*-indol-3-yl)-propionylamino]-pentanedioic Acid 5-Amide 1-(4-Carbamimidoyl-benzylamide) Trifluoroacetate (14) Compound **14** was synthesized from (*S*)-2-[(*R*)-2-ethanesulfonylamino-3-(5-propoxy-1*H*-indol-3-yl)-propionylamino]-pentanedioic acid 5-amide 1-(4-cyano-benzylamide) according the procedure described for **11** (83%, 98 mg). ^{1}H-NMR (270 MHz, CD_3OD) δ: 1.04 (3H, t, J=7.3 Hz), 1.10 (3H, t, J=7.4 Hz), 1.63—2.09 (6H, m), 2.69—2.92 (2H, m), 3.02—3.31 (2H, m), 4.01 (2H, t, J=6.6 Hz), 4.14—4.24 (2H, m), 4.39—4.57 (2H, m), 6.82 (1H, dd, J=2.3, 8.9 Hz), 7.14 (1H, d, J=2.3 Hz), 7.17 (1H, s), 7.27 (1H, d, J=8.9 Hz), 7.53 (2H, d, J=8.6 Hz), 7.76 (2H, d, J=8.2 Hz); HR-MS (ESI+) Calcd for $C_{29}H_{40}N_7O_6S$: 614.2755 (M^++1). Found: 614.2762.

5-(3-{(*R*)-2-[(*S*)-1-(4-Carbamimidoyl-benzylcarbamoyl)-3-carbamoyl-propylcarbamoyl]-2-ethanesulfonylamino-ethyl}-1*H*-indol-5-yloxy)-pentanoic Acid Trifluoroacetate (15) Compound **15** was synthesized from 5-(3-{(*R*)-2-[(*S*)-3-carbamoyl-1-(4-cyano-benzylcarbamoyl)-propylcarbamoyl]-2-ethanesulfonylamino-ethyl}-1*H*-indol-5-yloxy)-pentanoic acid ethyl ester according the procedure described for **11** and **16** (51%, 20 mg). ^{1}H-NMR (300 MHz, CD_3OD) δ: 1.02 (3H, t, J=7.4 Hz), 1.58—2.06 (8H, m), 2.41 (3H, dd, J=3.6, 6.8 Hz), 2.68—3.41 (4H, m), 4.02—4.10 (2H, m), 4.11—4.21 (2H, m), 4.37—4.54 (2H, m), 6.80 (1H, dd, J=2.3, 8.8 Hz), 7.13 (1H, d, J=2.2 Hz), 7.15 (1H, s), 7.24 (1H, d, J=8.8 Hz), 7.52 (2H, d, J=8.4 Hz), 7.74 (1H, d, J=8.4 Hz), 8.31—8.42 (2H, m); HR-MS (ESI+) Calcd for $C_{31}H_{42}N_7O_8S$: 672.2810 (M^++1). Found: 672.2806.

Crystal Structures. Cloning, Expression, Purification, and Crystallization Purified human FVIIa/sTF and crystals of human FVIIa/sTF in complex with compounds **2**, **14** and **16** were prepared as described previously.[21,24,27]

Data Collection After soaking in a cryoprotectant solution of 10% PEG 5000, 100 mM cacodylate buffer, pH 5.0, 100 mM NaCl, and 5 mM $CaCl_2$, 30% (v/v) glycerol, the crystals were frozen at 100 K in a nitrogen gas stream. X-Ray diffraction data on the FVIIa/sTF crystals in complex with compounds **2**, **14** and **16** were collected on an R-axis IV (Rigaku) mounted on a copper rotating-anode X-ray generator ultraX 18 (Rigaku) equipped with a Confocal Mirror (Osmic). The data were processed using Denzo and Scalepack software.[28]

Structure Determination and Refinement The crystals of FVIIa/sTF in complex with compound **16** were prepared as described previously.[24,27]

X-Ray diffraction data of this crystal was collected on an R-axis IV (Rigaku) mounted on a copper rotating-anode X-ray generator ultraX 18 (Rigaku) equipped with Confocal Mirror (Osmic) at 100 K. The data was processed using Denzo and Scalepack.

The model phases of FVIIa/sTF in complex with compounds **16** were improved by rigid body refinement with CNX (Accelrys), using the previously published structure of FVIIa/sTF in complex with D-Phe-Phe-Arg chloromethyl ketone (PDB code 1DAN)[29] as a starting model. The inhibitor molecules were identified using the difference Fourier method. A model of the protein and inhibitor was built with Quanta (Accelrys) and the structure was refined with CNX (Accelrys).

Biology. Human Factor VIIa (FVIIa) Inhibition Activity A 10% (v/v) DMSO solution of each test compound (20 μl) was mixed with 40 μl Thromborel S (50 mg/ml; Dade Behring), 20 μl Spectrozyme® FVIIa (CH_3SO_2-D-CHA-But-Arg-pNA·AcOH) (5 mM; American Diagnostica Inc.), 20 μl $MgCl_2$ (10 mM), 60 μl ethylene glycol, 20 μl buffer (500 mM Tris–HCl, pH 7.5, 1500 mM NaCl, 50 mM $CaCl_2$) and 40 μl distilled water in a 96-well assay plate. The reaction was initiated by the addition of 20 μl human FIXa solution (20 nM; Enzyme Research Laboratories) and then the absorbance at 405 nm was monitored to measure the initial velocity of the reaction. Percent inhibition at each concentration was calculated from the experimental and control samples. IC_{50} values were calculated from the concentration–reaction activity curve of each test compound.

Human Thrombin Inhibition Activity A 10% (v/v) DMSO solution of test compound (20 μl) was mixed with 40 μl buffer (200 mM Tris–HCl, pH

8.0), 20 μl NaCl solution (1 M), 20 μl FVR-pNA (2 mM; Sigma), and 80 μl distilled water in a 96-well assay plate. The reaction was initiated by the addition of 20 μl human thrombin solution (5 U/ml, Sigma) and then the absorbance at 405 nm was monitored to measure the initial velocity of the reaction. Percent inhibition at each concentration was calculated from the experimental and control sample. IC_{50} values were calculated from the concentration–reaction activity curve of each test compound.

Human Factor FIXa (FIXa) Inhibition Activity A 10% (v/v) DMSO solution of test compound (20 μl) was mixed with 20 μl Spectrozyme® FXa (MeO-CO-D-CHG-Gly-Arg-pNA·AcOH) (5 mM; American Diagnostica Inc.), 20 μl buffer (500 mM Tris–HCl, pH 7.5, 1500 mM NaCl, 50 mM $CaCl_2$) and 80 μl distilled water in a 96-well assay plate. The reaction was initiated by the addition of 20 μl human FVIIa solution (20 nM; Enzyme Research Laboratories) and then the absorbance at 405 nm was monitored to measure the initial velocity of the reaction. Percent inhibition at each concentration was calculated from the experimental and control sample. The IC_{50} value was calculated from the concentration–reaction activity curve of each test compound.

Human Factor Xa (FXa) Inhibition Activity A 10% (v/v) DMSO solution of test compound (20 μl) was mixed with 20 μl buffer (500 mM Tris–HCl, pH 8.4, 1500 mM NaCl), 20 μl S-2222 (Bz-Ile-Glu(γ-OR)-Gly-Arg-pNA·HCl) (5 mM; Daiichi Pure Chemical), and 120 μl distilled water in a 96-well assay plate. The reaction was initiated by the addition of 20 μl human FXa solution (50 mU/ml; Enzyme Research Laboratories) and the absorbance at 405 nm was then monitored to measure the initial velocity of the reaction. Percent inhibition at each concentration was determined from the experimental and control samples. The IC_{50} value was calculated from the concentration–reaction activity curve of each test compound.

Human Factor XIa (FXIa) Inhibition Activity A 10% (v/v) DMSO solution of test compound (20 μl) was mixed with 100 μl buffer (200 mM Tris–HCl, pH 7.2, 300 mM NaCl), 20 μl S-2366 (pyroGlu-Pro-Arg-pNA·HCl) (2 mM, Daiichi Pure Chemical), and 40 μl distilled water in a 96-well assay plate. The reaction was initiated by the addition of 20 μl human FXIa solution (5 nM, Enzyme Research Laboratories) and the absorbance at 405 nm was then monitored to measure the initial velocity of the reaction. Percent inhibition at each concentration was determined from the experimental and control samples. The IC_{50} value was calculated from the concentration–reaction activity curve of each test compound.

Human Factor XIIa (FXIIa) Inhibition Activity A 10% (v/v) DMSO solution of test compound (20 μl) was mixed with 100 μl buffer (200 mM Tris–HCl, pH 8.3, 300 mM NaCl), 20 μl S-2302 (1H D-Pro-Phe-Arg-pNA·2HCl) (2 mM, Daiichi Pure Chemical), and 40 μl distilled water in a 96-well assay plate. The reaction was initiated by the addition of 20 μl human FXIIa solution (50 nM, Enzyme Research Laboratories) and the absorbance at 405 nm was then monitored to measure the initial velocity of the reaction. Percent inhibition at each concentration was determined from the experimental and control samples. The IC_{50} value was calculated from the concentration–reaction activity curve of each test compound.

Human Activated Protein C (APC) Inhibition Activity A 10% (v/v) DMSO solution of test compound (20 μl) was mixed with 40 μl buffer (200 mM Tris–HCl, pH 8.0), 40 μl S-2366 (pyroGlu-Pro-Arg-pNA·HCl) (2 mM, Daiichi Pure Chemical), 20 μl NaCl (1 M), 20 μl $CaCl_2$ (20 mM), and 40 μl distilled water in a 96-well assay plate. The reaction was initiated by the addition of 20 μl human APC (1 μg/ml, Sigma) and the absorbance at 405 nm was then monitored to measure the initial velocity of the reaction. Percent inhibition at each concentration was determined from the experimental and control samples. The IC_{50} value was calculated from the concentration–reaction activity curve of each test compound.

Prothrombin Time (PT) One hundred microliters human plasma (Dade Behring) containing the test compound was incubated at 37 °C for 3 min and was then mixed with 100 μl Thromborel S (Dade Behring). The plasma clotting time was then measured using a KC-10A coagulometer (Amelung). The concentration for the two-fold prolongation of PT (2×PT) was calculated from the concentration–reaction activity curve of each test compound.

Activated Partial Thromboplastin Time (APTT) Human plasma (100 μl; Dade Behring) containing the test compound was incubated at 37 °C for 1 min and then mixed with 100 μl APTT reagent (Sigma). After 3 min, the human plasma was mixed with 100 μl $CaCl_2$ (20 mM). The plasma clotting time was then measured using a KC-10A coagulometer (Amelung). The concentration for the two-fold prolongation of APTT (2×APTT) was calculated from the concentration–reaction activity curve of each test compound.

Acknowledgments We thank Ms. Hitomi Suda of Chugai Pharmaceutical Co., Ltd. for HR-MS measurements of the compounds and Ms. Frances Ford of Chugai Pharmaceutical Co., Ltd. for proofreading the manuscript.

References

1) Davie E. W., Fujikawa K., Kisiel W., *Biochemistry*, **30**, 10363—10370 (1991).
2) Braunwald E., Califf R. M., Cannon C. P., Fox K. A., Fuster V., Gibler W. B., Harrington R. A., King S. B. 3rd, Kleiman N. S., Theroux P., Topol E. J., Van de Werf F., White H. D., Willerson J. T., *Am. J. Med.*, **108**, 41—53 (2000).
3) Himber J., Refino C. J., Burcklen L., Roux S., Kirchhofer D., *Thromb. Haemostasis*, **85**, 475—481 (2001).
4) Harker L. A., Hanson S. R., Wilcox J. N., Kelly A. B., *Haemostasis*, **26** (Suppl. 1), 76—82 (1996).
5) Suleymanov O. D., Szalony J. A., Salyers A. K., LaChance R. M., Parlow J. J., South M. S., Wood R. S., Nicholson N. S., *J. Pharmacol. Exp. Ther.*, **306**, 1115—1121 (2003).
6) Szalony J. A., Taite B. B., Girard T. J., Nicholson N. S., LaChance R. M., *J. Thromb. Thrombolysis*, **14**, 113—121 (2002).
7) Zoldhelyi P., McNatt J., Shelat H. S., Yamamoto Y., Chen Z. Q., Willerson J. T., *Circulation*, **101**, 289—295 (2000).
8) Kelley R. F., Refino C. J., O'Connell M. P., Modi N., Sehl P., Lowe D., Pater C., Bunting S., *Blood*, **89**, 3219—3227 (1997).
9) Miura M., Seki N., Koike T., Ishihara T., Niimi T., Hirayama F., Shigenaga T., Sakai-Moritani Y., Tagawa A., Kawasaki T., Sakamoto S., Okada M., Ohta M., Tsukamoto S., *Bioorg. Med. Chem.*, **15**, 160—173 (2007).
10) Young W. B., Mordenti J., Torkelson S., Shrader W. D., Kolesnikov A., Rai R., Liu L., Hu H., Leahy E. M., Green M. J., Sprengeler P. A., Katz B. A., Yu C., Janc J. W., Elrod K. C., Marzec U. M., Hanson S. R., *Bioorg. Med. Chem. Lett.*, **16**, 2037—2041 (2006).
11) Hu H., Kolesnikov A., Riggs J. R., Wesson K. E., Stephens R., Leahy E. M., Shrader W. D., Sprengeler P. A., Green M. J., Sanford E., Nguyen M., Gjerstad E., Cabuslay R., Young W. B., *Bioorg. Med. Chem. Lett.*, **16**, 4567—4570 (2006).
12) Zbinden K. G., Obst-Sander U., Hilpert K., Kuhne H., Banner D. W., Bohm H. J., Stahl M., Ackermann J., Alig L., Weber L., Wessel H. P., Riederer M. A., Tschopp T. B., Lave T., *Bioorg. Med. Chem. Lett.*, **15**, 5344—5352 (2005).
13) Schweitzer B. A., Neumann W. L., Rahman H. K., Kusturin C. L., Sample K. R., Poda G. I., Kurumbail R. G., Stevens A. M., Stegeman R. A., Stallings W. C., South M. S., *Bioorg. Med. Chem. Lett.*, **15**, 3006—3011 (2005).
14) Sagi K., Fujita K., Sugiki M., Takahashi M., Takehana S., Tashiro K., Kayahara T., Yamanashi M., Fukuda Y., Oono S., Okajima A., Iwata S., Shoji M., Sakurai K., *Bioorg. Med. Chem.*, **13**, 1487—1496 (2005).
15) Riggs J. R., Hu H., Kolesnikov A., Leahy E. M., Wesson K. E., Shrader W. D., Vijaykumar D., Wahl T. A., Tong Z., Sprengeler P. A., Green M. J., Yu C., Katz B. A., Sanford E., Nguyen M., Cabuslay R., Young W. B., *Bioorg. Med. Chem. Lett.*, **16**, 3197—3200 (2006).
16) Rai R., Kolesnikov A., Sprengeler P. A., Torkelson S., Ton T., Katz B. A., Yu C., Hendrix J., Shrader W. D., Stephens R., Cabuslay R., Sanford E., Young W. B., *Bioorg. Med. Chem. Lett.*, **16**, 2270—2273 (2006).
17) Groebke Zbinden K., Banner D. W., Hilpert K., Himber J., Lave T., Riederer M. A., Stahl M., Tschopp T. B., Obst-Sander U., *Bioorg. Med. Chem.*, **14**, 5357—5369 (2006).
18) Shiraishi T., Kadono S., Haramura M., Kodama H., Ono Y., Iikura H., Esaki T., Koga T., Hattori K., Watanabe Y., Sakamoto A., Yoshihashi K., Kitazawa T., Esaki K., Ohta M., Sato H., Kozono T., *Bioorg. Med. Chem. Lett.*, **18**, 4533—4537 (2008).
19) Shiraishi T., Kadono S., Haramura M., Kodama H., Ono Y., Iikura H., Esaki T., Koga T., Hattori K., Watanabe Y., Sakamoto A., Yoshihashi K., Kitazawa T., Esaki K., Ohta M., Sato H., Kozono T., *Lett. Drug Des. Discov.*, **6**, 86—92 (2009).
20) Kadono S., Sakamoto A., Kikuchi Y., Oh-Eda M., Yabuta N., Yoshihashi K., Kitazawa T., Suzuki T., Koga T., Hattori K., Shiraishi T., Haramura M., Kodama H., Ono Y., Esaki T., Sato H., Watanabe Y., Itoh S., Ohta M., Kozono T., *Biochem. Biophys. Res. Commun.*, **326**, 859—865 (2005).
21) Kadono S., Sakamoto A., Kikuchi Y., Oh-eda M., Yabuta N., Yoshihashi K., Kitazawa T., Suzuki T., Koga T., Hattori K., Shiraishi T., Haramura M., Kodama H., Ono Y., Esaki T., Sato H., Watanabe Y., Itoh S., Ohta M., Kozono T., *Biochem. Biophys. Res. Commun.*, **327**,

589—596 (2005).
22) Kadono S., Sakamoto A., Kikuchi Y., Oh-Eda M., Yabuta N., Koga T., Hattori K., Shiraishi T., Haramura M., Kodama H., Ono Y., Esaki T., Sato H., Watanabe Y., Itoh S., Ohta M., Kozono T., *Acta Crystallogr. Sect. F: Struct. Biol. Cryst. Commun.*, **61**, 169—173 (2005).
23) Kadono S., Sakamoto A., Kikuchi Y., Oh-eda M., Yabuta N., Koga T., Hattori K., Shiraishi T., Haramura M., Kodama H., Esaki T., Sato H., Watanabe Y., Itoh S., Ohta M., Kozono T., *Lett. Drug Des. Discov.*, **2**, 165—171 (2005).
24) Kadono S., Sakamoto A., Kikuchi Y., Oh-eda M., Yabuta N., Koga T., Hattori K., Shiraishi T., Haramura M., Kodama H., Esaki T., Sato H., Watanabe Y., Itoh S., Ohta M., Kozono T., *Biochem. Biophys. Res. Commun.*, **324**, 1227—1233 (2004).
25) Shiraishi T., Kadono S., Haramura M., Sato H., Kozono T., Koga T., Sakamoto A., Japan Patent WO02062829A1 (2002).
26) Bode W., Mayr I., Baumann U., Huber R., Stone S. R., Hofsteenge J., *EMBO J.*, **8**, 3467—3475 (1989).
27) Kirchhofer D., Guha A., Nemerson Y., Konigsberg W. H., Vilbois F., Chene C., Banner D. W., D'Arcy A., *Proteins*, **22**, 419—425 (1995).
28) Otwinowski Z., Minor W., *Methods Enzymol.*, **276**, 307—326 (1997).
29) Banner D. W., D'Arcy A., Chene C., Winkler F. K., Guha A., Konigsberg W. H., Nemerson Y., Kirchhofer D., *Nature* (London), **380**, 41—46 (1996).